

ARTIFICIAL INTELLIGENCE APPLICATION IN PHOTOACOUSTIC OF GASES

UDC 007.52:543.52

Mladena Lukić¹, Žarko Čojbašić², Dragan D. Markushev³

¹Faculty of Occupational Safety, University of Niš, Niš, Serbia

²Mechanical Engineering Faculty, University of Niš, Niš, Serbia

³Institute of Physics, National Institute of the Republic of Serbia,
University of Belgrade, Beograd-Zemun, Serbia

Abstract. *Photoacoustic spectroscopy is a powerful, non-destructive, ultrasensitive technique that covers a wide range of applications including atmospheric monitoring, industrial, environmental, and biomedical practice. In this paper, our attention is focused on the area of artificial intelligence implementation in photoacoustic spectroscopy of gases. Artificial intelligence has been proven as a very successful, effective, and promising method for the accurate and real-time determination of photoacoustic signal parameters, related to relaxation, thermal and other physical properties of various media (i.e., for solving the inverse photoacoustic problem). To improve the sensitivity and selectivity of the photoacoustic method feedforward multilayer perceptron network is applied for real-time simultaneous determination of photoacoustic signal parameters: vibrational-to-translational relaxation time, and radius of the laser beam. Also, to solve the problem of finding optimal values of these photoacoustic parameters, metaheuristic algorithms, genetic algorithms and simulated annealing are used. The performance of artificial intelligence methods has been tested on a set of experimental signals generated in the (SF₆+Ar) gas. The potential advantages and disadvantages of those methods are discussed.*

Key words: *photoacoustic spectroscopy, artificial neural network, vibration to translation relaxation time, laser beam radius, genetic algorithms, simulated annealing.*

1. INTRODUCTION

Photoacoustic spectroscopy (PAS) is a laser-based, ultrasensitive technique applicable to samples in all aggregate states. The first successful PAS application was performed by Kreuzer in 1971, for the detection of low gas concentration [1]. During this time PAS has

Received March 8, 2023 / Accepted March 27, 2023

Corresponding author: Mladena Lukić

University of Niš, Faculty of Occupational Safety, Čarnojevića 10a, 18000 Niš, Serbia

E-mail: mladena.lukic@znrfak.ni.ac.rs

been established as a powerful technique with high detection sensitivity (of 1 pptv -10^{-12} or even ppqv -10^{-17} concentration), high selectivity, multicomponent capability, and large dynamic range [2, 3, 4, 5]. PAS is based on the sensitive detection of acoustic waves which are generated in a sample after absorption of pulsed or modulated laser radiation. Absorbed energy is released as heat via the nonradiative relaxation channel. Small, local, temperature variations cause pressure variations detected by an appropriate detector. PAS is widely used as a tool for the determination of the optical and thermal properties of gases, liquids, and solids. In the past decades, PAS has been recognized as an effective technique for the measurement of trace gas concentration, whereby the concentration of the absorbing component can be calculated from the optical absorption. Nowadays trace gas monitoring is of keen interest considering their role in radiative disbalance in the Earth-atmosphere system and the emergence of different phenomena such as: rapid increase of global temperature, ice melting, snow cover decreasing, changes in weather patterns, storm intensities, etc. Except for air pollution and climate, the sensitive and selective detection and monitoring of trace gases is important for numerous research areas: agriculture and food industry, industrial processes, and workplace safety. Also, the photoacoustic (PA) method has growing applications in medical imaging, photochemistry, chemical reactions dynamics, interface ultrasonic waves, studies of nonequilibrium transport of heated electrons in metals, investigation of semiconductors properties, non-contact characterization, generation of acoustic solitons in crystals, soft matter research, etc. [6]. In investigations of solid and liquid samples, it has demonstrated advantages over traditional conventional spectroscopy, particularly for weakly absorbing, strongly scattering, opaque samples, diffusing samples, thin films, or multilayered structures. [2].

The main parts of the PAS experimental setup for gas sensing are the radiation source (laser), PA cell and detector. The sensitivity of a PA system depends on exciting laser power, the sensitivity of the microphone, the cell constant, and the molar absorption coefficient of the analyte [7]. The capacitive microphone is a common sensing element used in PAS. However, its usage isn't convenient in explosive environments, under high temperatures, and under electromagnetic influences. To improve the sensitivity of the PAS system and enhancing signals to noise ratio, different methods are proposed related to the laser power increase, acoustic cell, and detector improvement [8]. Recently, a number of successful alternatives to capacitive microphones have been developed and put into use: optical sensors (uncharged and highly sensitive), resonant tuning forks (QTF) (with small size, environmental noise immunity, and corrosion resistance) [9, 10], miniature silicon or micromechanical cantilever (extended dynamic range) [11, 12], etc. Unlike the mentioned methods, and based on our previous research, we will review artificial intelligence (AI) applications in PAS that proved as effective tools to achieve better precision and real-time operation with no changes in experimental setup [13, 14, 15, 16, 17]. Recently, the growing interest in deep learning neural network applications is noticeable in many techniques based on the PA method and inverse problem solving (mainly in photoacoustic imaging - PAI) [18].

In this article, we present theoretical background regarding inverse problem solving, followed by our results for AI application for simultaneous determination of PA signal parameters: the laser beam spatial profile $R(r_L)$, vibrational-to-translational relaxation time τ_{V-T} , and distance from the laser beam to the absorption molecules in the photoacoustic cell r^* . Our results suggest that the application of artificial neural networks (ANNs) may improve the sensitivity and selectivity of the PA detection method providing high

precision, and the opportunity for application for higher intensities of radiation. Also, metaheuristic algorithms (genetic algorithms -GA and simulated annealing - SA) can be considered an important method for problem optimization ensuring high accuracy and the ability to search for unknown signal parameters in a wide parameter range. AI implementation within photoacoustic may increase the efficiency and dynamic range of the measurement, and relieve in situ manipulation with instruments.

2. THEORETICAL BACKGROUND

The shape and intensity of the PA signal are the main quantities that can be analyzed in the time domain. Absorbed laser energy is converted into heat via a nonradiative relaxation channel. Molecular relaxation is performed through energy transfer processes between different modes of the molecule. The dominant type of energy transfer for polyatomic molecules is a transfer between vibrational and translational modes, known as vibrational-to-translational relaxation (or V-T relaxation), characterized by vibrational-to-translational relaxation time τ_{V-T} . The temporal shape of the PA signal (obtained for pulsed laser excitation) is a function of τ_{V-T} , and can be calculated by solving the nonhomogeneous linearized wave equation [19, 20, 21]:

$$\frac{\partial^2 \delta p(\mathbf{r}, t)}{\partial t^2} - c^2 \Delta \delta p(\mathbf{r}, t) = S(\mathbf{r}, t) \quad (1)$$

where $\delta p(\mathbf{r}, t)$ is the pressure discrepancy from its equilibrium value, c is the speed of sound and $S(\mathbf{r}, t)$ is the source function.

If the distribution of excited molecules at location \mathbf{r} and time t are given by some energy release rate function $E(\mathbf{r}, t)$, then the source function in equation (1) is defined as:

$$S(\mathbf{r}, t) = -\frac{\partial^2 E(\mathbf{r}, t)}{\partial t^2} H(t) - \frac{\partial E(\mathbf{r}, t)}{\partial t} \delta(t) \quad (2)$$

where $H(t)$ is the Heaviside step function and $\delta(t)$ is the Dirac delta function.

Wave equations can be solved by Fourier transform method and Green's functions method, for known source functions and defined initial and boundary conditions. Fourier transform method is suitable for simple spatial profiles of the laser beam (top hat, Gaussian, Lorentz, etc.), cylindrical symmetry, and the exponential decays of the excitation energy [19], while Green's functions method is more applicable for arbitrary spatial laser beam profile and energy decay [20]. For known simple spatial profiles of the laser beam, the solution of the nonhomogeneous linearized wave equation (1) obtained by the Fourier transform method are PA signals given in the form:

$$\delta p(r^*, t^*) = \frac{RE_0}{C_V V} \int_0^\infty (l^2 + \varepsilon^2)^{-1} [-\varepsilon \exp(-\varepsilon t^*) + l \sin lt^* + \varepsilon \cos lt^*] J_0(lr^*) h(l) dl \quad (3)$$

PA signal $\delta p(r^*, t^*)$ is determined by: universal gas constant R , absorbed energy E_0 , irradiated volume V , and molar heat capacity at constant volume C_V , $l = kr_L$ (k is a wave vector, and r_L is a radius of a spatial profile of laser beam). J_0 are the first-kind Bessel

functions of zero order and $h(l)$ is a function that depends on the spatial profile of the excitation radiation (top hat, Gauss, Lorentz profile).

The general solution of the linearized wave equation (1) using the method of Green's functions [20] for exponential decay of the excitation energy can be written in the form:

$$\begin{aligned} \delta p(\mathbf{r}, t) &= \int d^3 \mathbf{r}' \int dt' g(\mathbf{r}, t | \mathbf{r}', t') S(\mathbf{r}', t') = \\ &= \delta p(r, t) = -\frac{\partial T(0)}{\partial t} G(r, t) - \int_0^t \frac{\partial^2 T}{\partial t'^2} G(r, t - t') dt' \end{aligned} \quad (4)$$

where $g(\mathbf{r}, t | \mathbf{r}', t')$ is Green's function for the two-dimensional wave equation. For cylindrical geometry, Green's function has the form:

$$g(\mathbf{r}, t | \mathbf{r}', t') = (2\pi c)^{-1} (c^2 (t - t')^2 - |\mathbf{r} - \mathbf{r}'|^2)^{-1/2} \quad (5)$$

and $G(r, t - t')$ is the Green's function averaged over the coordinate. The averaging gives:

$$G(r, t - t') = \frac{1}{2\pi c} \int_0^{2\pi} d\theta \int_0^r \frac{R(r') r' dr'}{[(t - t')^2 - r^2 + (2r \cos \theta) r' - r'^2]^{1/2}} \quad (6)$$

where r and θ are the cylindrical coordinates. In general, the energy release rate $E(\mathbf{r}, t)$ depends on the radius vector and time.

For cylindrical symmetry of the experiment, it depends on radial coordinates and time $E(\mathbf{r}, t) = E(r, t)$. The energy release function $E(r, t) = R(r) T(t)$ can then be divided into two parts: spatial $R(r)$ (dependent on the coordinate and geometric properties of the laser beam) and temporal $T(t)$ (describing molecular relaxation).

Calculation of theoretical PA signal might be more efficient introducing dimensionless parameters r^* and t^* known as the reduced coordinate and the reduced time, instead of coordinate r and time t . Reduced coordinate r^* represents the distance from a laser beam to a detector (microphone) and defines as $r^* = r/r_L$, where r is the radial coordinate, and r_L is the laser beam radius. Reduced time can be written as $t^* = t/\tau_p$, where t is the time, τ_p is a sonic transit time ($\tau_p = r_L/c$), c is the speed of sound. The shape and intensity of PA signals are specified by a dimensionless parameter ($\varepsilon = r_L/c\tau_p$). Figure 1 shows the dependences of intensity and shape of PA signal on quantity ε , for four different spatial laser beam profiles. Calculated theoretical signals are compared to experimental signals generated in an SF₆+Ar gas mixture. Sulphur hexafluoride (SF₆) as a greenhouse gas has a huge potential for climate impact in the future, due to its strong infrared (IR) absorption, long atmospheric lifetime (3,200 years) and high global warming potential (GWP) of 23,900 calculated over 100-year time horizon [22]. It is a human-made, powerful greenhouse gas emitted by a variety of industrial processes including aluminum melting, electric power transmission and distribution, magnesium processing, and semiconductor manufacturing.

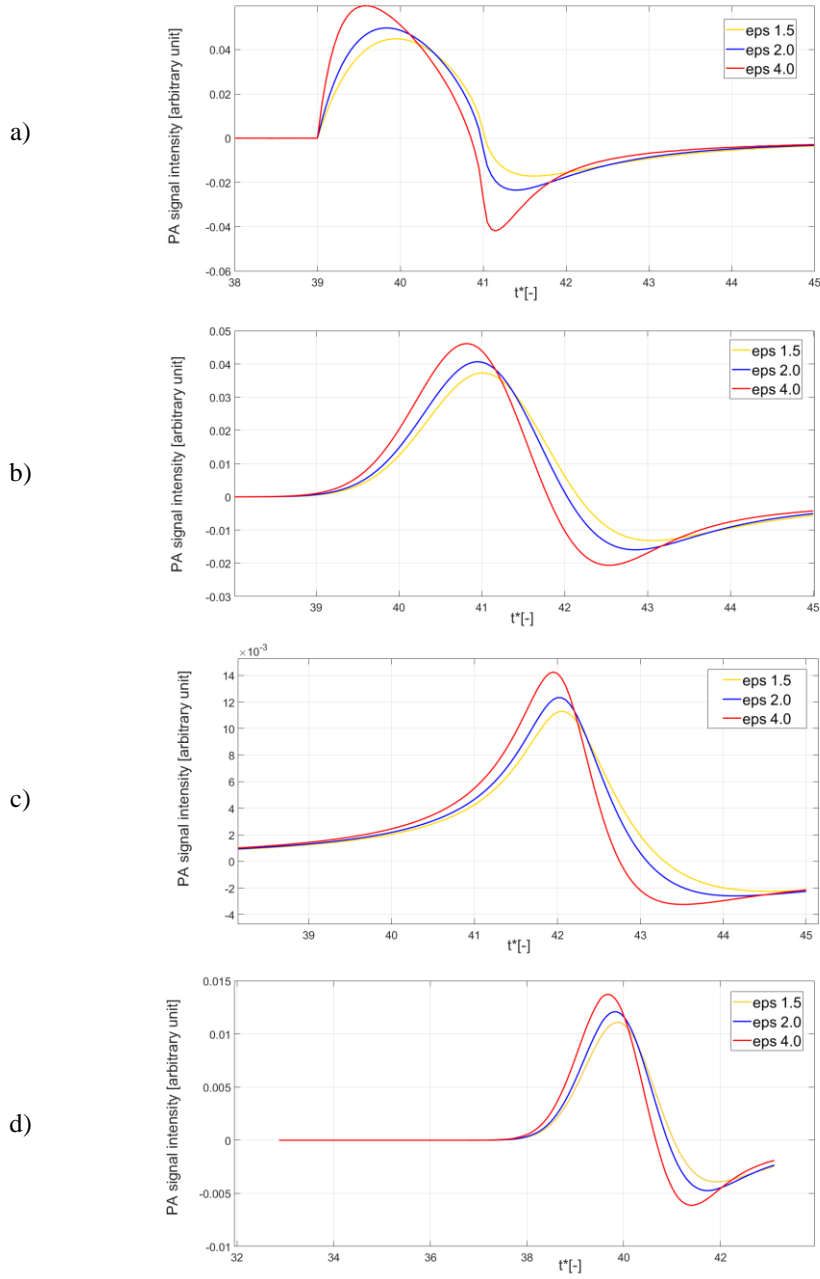


Fig. 1 Theoretical PA signals for a) top hat, b) Gauss, c) Lorentz and d) Lorentz, with a hole spatial laser beam profile, calculated for three different ϵ values (1.5, 2.0 and 4.0). Shape and intensity of PA signals are defined by parameter ϵ .

Our experimental pulsed PAS setup for the gas sample examination and relaxation time measurements consisted of the laser, cell, and microphone. As a radiation source a tunable pulsed CO₂ laser (TEA CO₂) (FWHM 45 ns, fluence of 1 J/cm², repetition rate ~ 1 Hz) with maximum laser power over 10 MW multimode and 4 MW in TEM₀₀ mode, is used. The nonresonant cell contained the investigated gas mixtures SF₆+Ar at the total pressures of $p_{total} = 10 - 100$ mbar and the absorber pressure $p_{abs(SF_6)} = 0.47$ mbar. Acoustic waves are detected by a capacitive microphone Knowles Electronic Co., model 2832. Also, we used some optics (beam splitters, lenses) and additional instrumentation (power meters, vacuum meters, oscilloscopes, beam profilers) [23,24].

3. ARTIFICIAL INTELLIGENCE APPLICATION IN PHOTOACOUSTICS OF GASES

Photoacoustic method for the detection of atmospheric pollutants is based on non-radiative molecular relaxation and the determination of vibrational-to-translational relaxation time τ_{v-T} [25]. Relaxation time τ_{v-T} is an important molecule feature that could be used as criterion for the determination of various molecular species. Many quantities such as energy transfer collisional rate, energy transfer probability, and collisional cross-section, are τ_{v-T} relaxation time dependent. Furthermore, this quantity could be used as a basic parameter for different models of energy transfer in the atmosphere [22]. Finding a reliable method for determination of τ_{v-T} is a particularly challenging task, due to its dependence on the spatial profile of the laser beam [26, 27]. It has been shown experimentally and theoretically [23, 24] that even small variations in the laser beam spatial profile of the high-power laser significantly affect τ_{v-T} values. Further, errors in τ_{v-T} determination can lead to the reduction of selectivity and sensitivity of PAS measurement. It is very common for the device performances of various commercial instruments for precise determination of the spatial profile of the laser beam to degrade during the use of high-power lasers [28, 29]. Also, for in situ measurement additional optical instruments (such as a beam profiler) are not convenient and may introduce errors in measurements. Conventional algorithms for inverse problem solving and laser beam profile reconstruction (back-projection, exact solution, Fourier, Greens' function), although provide exact solutions for PA signal parameters, are very time consuming, and can be used only as a corrective procedure after the completed experiment. To support real-time operation and overcome problems with simultaneous determination of τ_{v-T} and spatial laser beam profile, we applied artificial neural networks (ANNs), and two metaheuristic algorithms: genetic algorithms (GA) and simulated annealing (SA). Metaheuristic algorithms are useful tools for parameter estimation, particularly in a dynamic and changeable environment, and under limited knowledge of problems to be solved [13, 14, 30].

3.1. Artificial neural networks for simultaneous determination of photoacoustic signal parameters

Artificial neural networks (ANNs) are a model of the human brain consisting of nodes (neurons), connections, and transfer functions [31, 32]. To calculate the simultaneous and real-time spatial profile of the laser beam $R(r)$ (namely the class of laser beam profile), r^* (the distance where PA signal is calculated) and vibrational-to-translational relaxation time τ_{v-T} , feed-forward multilayer perception (MLP) networks are trained in an offline

batch training regime. Between the input and output layers, an MLP has one or more hidden layers of neurons. Using input-output training data MLP learns the representation by exploiting the error backpropagation (BP) algorithm. The error (difference between the desired signal and the network output) propagates backward through the network, establishing a closed-loop control system [31]. Connections between layers of neurons (weights) are adjusted using the BP algorithm. To prevent network overfitting and achieve good generalization capability dataset is divided into a training set, a validation set and a test set. Network inputs were PA signals sampled in 21 or 28 equidistant points over the interval. Network outputs consisted of three nodes that estimated three parameters: a reduced coordinate r^* parameter ε and a class of spatial laser beam profiles. Profile shape class distinguishes Gauss, top hat, and Lorentz profiles. The number of hidden layers and the number of processing elements per hidden layer are selected through many trial-and-error processes, representing a trade-off between network complexity, precision, and execution time. It has been shown that MLP network architectures with 21 or 28 inputs, and one or two hidden layers (having 7 to 15 nodes), produce satisfactory good estimations of PA signal parameters with acceptable accuracy and computational cost. Theoretical PA signals (Figure 2) are calculated by Fourier [33] and Green's function method [34, 13]. Using Green's function method, theoretical PA signals for a more realistic spatial laser beam profile - Lorentz with a hole have been calculated. According to our experimental conditions [23, 24] parameter r^* (or distance between laser and detector) for each profile shape, had values of 39, 40, 41, and 42. For each r^* value, ε has values in the range (0.5 to 5). A dataset of 120 PA signals is calculated and divided into a training (84 PA signals) set, a validation set (18 PA signals) and a test set that has no effect on training (18 PA signals). Since our aim was to find an appropriate, effective method that can improve in situ PAS performances, we compared the results of three network topologies that differ by the number of neurons in one hidden layer (10 or 15) and by a number of hidden layer (two layers with 7 neurons each). Further, we tested network performances with 21 input nodes (PA signals sampled in 21 points). Fewer nodes in the input layers can be an advantage for in situ measurements implying simpler PA signal preparation, reduced network complexity, and shorter execution time.

Also, we used a wider range of the parameter $\varepsilon \in [0.5 - 5]$, a larger dataset (240 PA signals divided into 168 signals for training, and 36 signals for validation and test set each), and a more realistic spatial beam profile (Lorentz with a hole), to check network performances [13].

For molecules, SF_6 in a gas mixture with Ar as a buffer gas, relaxation time τ_{v-T} , has an order of magnitude 10^{-6} s. Results for each created network are given in the range of $10 \mu\text{s}$. It can be concluded that the application of ANNs satisfies real-time operation and allows correction of spatial laser beam profile between two consecutive laser pulses. In the practical realization of the ANNs method, some problems with signals overlapping may occur. PA signals originating from different molecules can overlap for certain values of the parameter ε . Our results have shown better precision for parameter r^* (0.1% of the mean relative error), than parameter ε (3% of the mean relative error) [35]. Theoretical signals for different r^* are clearly separated but signals for certain values of the parameter ε can overlap, due to the nature of the vibrational-to-translational processes [36]. For in situ measurements, differentiation of signals can be achieved by laser excitation on the highest absorption lines of the investigated molecules, as well as by a different spatial

profile of the laser radiation. Further, our results for molecule C_2H_4 suggest that the application of another network type with fixed topology (radial bases neural networks-RBNNs), enables better precision in parameter ε prediction [37].

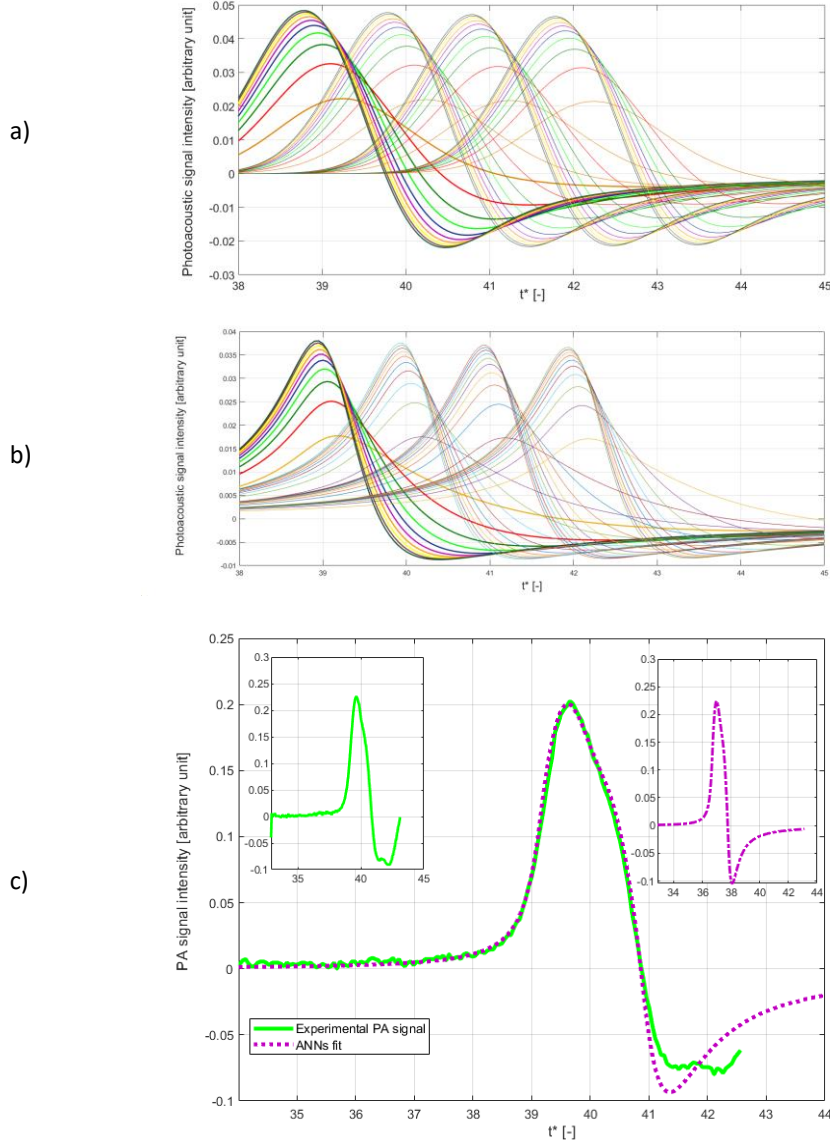


Fig. 2 Part of the training set (40 PA signals) obtained for a) Gauss profile shape and b) Lorentz profile shape for parameters $\varepsilon \in [0.5 - 5]$ and $r^* \in [39,30,41,42]$. c) experimental signal and ANNs fitted (theoretical) PA signal for more realistic spatial laser beam radius - Lorentz with a hole.

3.2. Metaheuristic algorithms for simultaneous determination of photoacoustic signal parameters

Photoacoustic spectroscopy relies on different conventional optimization methods. Two important applications are the calibration of the PAS system and the determination of concentrations of atmospheric pollutants. It was shown in [26] that with the standard Levenberg-Marquardt algorithm, it is possible to determine the PA signal parameters (r^* and ε) accurately. However, this implies an appropriate selection of initial parameters which is a very demanding task for real-world problems. Metaheuristic allows us to deal with large-size problem examples by delivering satisfactory solutions in a reasonable time. We chose two different metaheuristic algorithms for solving the problem of simultaneous determination of r_L and τ_{v-T} : genetic algorithms (GAs) and simulated annealing (SA). Our aim was to select the technique that meets the most of requirements for in situ measurement (sensitivity, selectivity, easy handling, wide dynamic range, low computational cost, etc.). Selected algorithms differ by natural processes which imitate (biological and physical), method of searching solution space (single solution or population), operators that use, etc.

A GAs is modelled on natural evolution, and the operators it employs are inspired by the natural evolution [38, 39, 40]. GAs provides solutions using randomly generated strings (chromosomes) that make the population in the potential solutions space. Real-coded genetic algorithms (RCGAs) were used due to simpler coding and decoding processes. In RCGAs, information is stored in the chromosome and represented by real numbers. Each chromosome has its own fitness value, which is a measure of the goodness of the solution. A chromosome with a higher fitness value is more likely to pass down to the next generation. Beside chromosome representation, the implementation of GAs requires the determination of the following issues: genetic operators, initialization, termination, and evaluation function. Genetic operators transform a set of chromosomes into sets with higher fitness values. The basic search mechanism of the GA is provided by the two types of operators: crossover and mutation, which are used to produce new solutions from individuals in the current population. RCGAs are used for problem-solving by fitting the experimental PA signal with the best-matching theoretical one. In considered optimization techniques, the objective function χ^2 (function to be optimized) is defined by the sum of the squared deviations of the experimental (simulated) and theoretical signals. When the value of χ^2 reaches the minimum, the values of parameters r^* and ε approach their optimal values. The experimental PA signal is simulated by the theoretical one, calculated by the Furie method for the Gaussian, top hat, or Lorentzian profile [13].

Unlike GAs, the simulated annealing (SA) algorithm is a single solution-based algorithm. The algorithm simulates evolution to the thermal equilibrium of a solid at a given temperature [41]. It is based on analogy between finding global optimum of given function and achieving stable configuration of a physical system. The temperature in the SA algorithm is a control parameter and gradually decreases during the optimization process (according to the cooling schedule), until the equilibrium (optimal) state is reached. Cooling schedule includes parameters setting: an initial temperature, a temperature update rule, the number of iterations to be performed and a stopping criterion [40, 42]. Selection of objective function and appropriate solutions representation are particularly important issues regarding the efficiency of the SA algorithm. A second important result of physics used in SA optimization is Boltzmann distribution - at a given temperature T , the probability that the system is in a state with energy E is determined by the: $P = e^{-E/k_B T}$, where P is the probability, E is energy, T is

temperature and k_B is Boltzmann's constant. The quality of SA prediction depends on the important parameter, initial temperature T_i selected mostly through many trial-and-error processes. Solution acceptance is based on another important parameter - reannealing. Reannealing is a step in the SA algorithm that defines the dynamics of worse solutions acceptance and prevents the algorithm to be "stuck" in the local minimum. For solving the problem of PA signal parameters determination, an optimal value of reannealing was 100. Theoretically, algorithm stops when the temperature becomes zero and further changes are not possible. In practice, when the value of the objective function χ^2 reaches the minimum and doesn't improve further, the algorithm stops. As a stopping criterion, we used a maximum number of evaluations of the objective function (1000). A hybrid function `Fmincon` is applied to improve the quality of the solution. An algorithm estimates unknown parameters of simulated PA signal for the Gauss profile shape with parameters $r^* = 40$ and $\varepsilon = 3.20$. The best-estimated parameter values were $r^* = 40$ and $\varepsilon = 3.20$. The choice of starting point has no effect on solution accuracy. It was confirmed that the SA algorithm with carefully selected parameters, provides accurate prediction of parameters, despite a broadly defined parameters range and starting point [30]. Table 1 shows the influence of algorithms parameters for several GAs and SA runs. The range of parameters (r^* and ε) was the same for both algorithms. The lower and upper limits of the parameters represent the smallest and largest values that can be expected under our experimental conditions and experimental setup. GAs for each individual in the population (each parameters pair), calculates the theoretical PA signal (for Gaussian, top hat, or Lorentzian profile) and objective function χ^2 . The number of generations is used as a stopping criterion for GAs search. It is obvious that for larger population size, GAs produces better results, but even in the case of a moderate number of generations and for a wider searching space, GAs can fit the experimental signal very precisely. Unlike ANNs which provide real-time operation, metaheuristic algorithms can be very time-consuming, but demonstrate high precision of simultaneous parameter determination in a wide parameter range.

Table 1 Comparison of GAs and SA prediction of parameters r^* and ε of unknown spatial laser beam profile.

GENETIC ALGORITHMS					
Lower and upper limits of r^* and ε	Parameters of algorithm				
	Exact solution	Algorithms prediction	Population size	Selection	Crossover
[10,0.2] [50, 4]	[40.00, 3.20]	[39.99, 3.14]	40	Roulette	Scattered
[10,0.2] [50, 4]	[41.10, 2.40]	[41.09, 2.39]	50		
[10,0.2] [50, 4]	[40.70, 0.90]	[40.70, 0.90]	70		
[10,0.2] [50, 4]	[42.20, 3.70]	[42.20, 3.70]	70		
SIMULATED ANNEALING					
Lower and upper limits of r^* and ε	Parameters of algorithm				
	Exact solution	Algorithms prediction	Starting point	Initial temperature	Reannealing
[10,0.2] [50, 4]	[40.00, 3.20]	[40.19, 2.91]	[30, 4]	50	100
[10,0.2] [50, 4]		[39.99, 2.82]	[30, 4]	50	80
[10,0.2] [50, 4]		[40.23, 2.99]	[30, 4]	60	100
[10,0.2] [50, 4]		[40.00, 3.20]	[30, 4]	60	100
[10,0.2] [50, 4]		[40.00, 3.20]	[39, 3.5]	60	100
[10,0.2] [50, 4]		[40.00, 3.20]	[20, 1]	60	100

Simulated annealing as single solution-based metaheuristics starts with a single solution and improves it. In the SA, the most important parameter is temperature, which determines the distance between points in the searching space (solutions), and the probability of solution acceptance. Initial temperature and reannealing have a significant impact on SA estimation, as population size and generation number in GAs run. For the simultaneous determination of PA parameters, SA has shown great effectiveness. It has fewer adjustable parameters, simpler structures, and low computational cost, all of which can be significant advantages for in situ measurement.

4. CONCLUSION

The main goal of this research was to find a method for PA trace gases in situ analysis that support recognizable potentials of PA detection such as sensitivity, selectivity, wide dynamic range, etc. Nowadays, easy-handling devices, capable to monitor and detect a changeable concentration of trace gases in a dynamic environment are the focus of scientific research. In this paper, we proposed intelligent techniques capable to learn and adapt to the environment. The sensitivity of PAS can be improved by real-time determination of experimental parameters, such as the radius of the spatial profile of the laser beam and profile class shape. Unknown spatial laser beam profiles and PA signal parameters (as relaxation time) can be detected from experimental PA signals, increasing the sensitivity and selectivity of the PAS methods. Relaxation time is a molecular characteristic and reliable criterion for the distinction of molecular species. By knowing vibrational-to-translational relaxation time with high precision, various molecule species can be detected with the same instrument. Using an intelligent technique parameter r^* , it is possible to calculate with extreme accuracy the capability to detect pollutants in distant layers of the atmosphere.

According to our results, it can be concluded that ANNs have a huge potential for PAS application in terms of precision and real-time operation. However, ANN training and topology selection through a trial-and-error process can be very time-consuming. Also, providing sufficient and valuable experimental data for ANN training under some circumstances, may be a problem.

Evaluation of metaheuristic algorithms prediction is performed by analysing solution quality, number of iterations, number of function evaluations, and robustness [43]. Also, other aspects such as simplicity, easy handling and flexibility were included. GAs for simultaneous determination of r^* and ε is proved as accurate and reliable, but are time-consuming due to a large number of function evaluations. Setting parameters that define the flow of artificial evolution can be a problem for in situ applications. GA is a robust method, which requires many function evaluations and more computational memory. However, due to its unique characteristics and effectiveness, GA may be a better option than other metaheuristic algorithms for optimizing a complex function in a large searching space. Algorithm SA with properly adjusted parameters has shown great potential for the simultaneous determination of PA signal parameters, reaching optimal solutions with a small number of function evaluations. Even though there are different experiences in SA application, it has shown remarkable efficiency in comparison with more complex GAs. For precise determination of unknown parameters, SA performs a small number of function evaluations that indicate greater efficiency for solving defined task - in situ measurements. The intelligent photoacoustic approach suggested here may serve as a framework for a wider range of AI applications and the development of adaptable systems for trace gas monitoring with a self-correction capability.

REFERENCES

1. L. B. Kreuzer and C. K. N. Patel, Nitric Oxide Air Pollution: Detection by Optoacoustic Spectroscopy, *Science*, 173 (3991), 45-47 (1971). DOI: 10.1126/science.173.3991.45.
2. M. Bertolotti, R. L. Voti, A note on the history of photoacoustic, thermal lensing, and photothermal deflection technique, *Journal of Applied Physics*, 128, 230901, (2020). DOI: 10.1063/5.0023836.
3. M.W. Sigrist, R. Bartlome, D. Marinov, J.M. Rey, D.E. Vogler, H. Wachter, Trace gas monitoring with infrared laser-based detection schemes, *Applied Physics B*, 90, 289–300 (2008). DOI: 10.1007/s00340-007-2875-4
4. T. Tomberg, M. Vainio, T. Hieta, L. Halonen, Sub-parts-per-trillion level sensitivity in trace gas detection by cantilever-enhanced photo-acoustic spectroscopy, *Scientific Reports* 8, 1848, (2018). DOI:10.1038/s41598-018-20087-9
5. L. Xionga, W. Baia, F. Chenb, X. Zhao, F. Yu, G.J. Diebold, Photoacoustic trace detection of gases at the parts-per-quadrillion level with a moving optical grating, *The Proceedings of the National Academy of Sciences*. 114, 7246-7249 (2017). DOI:10.1073/pnas.170604011
6. R. Anufriev, C. Glorieux, G. Diebold, Advances in photothermal and photoacoustic metrology, *Journal of Applied Physics* 128, 240402 (2020). DOI:10.1063/5.0039077
7. Z. Bozoki, A. Pogany, G. Szabo, Photoacoustic Instruments for Practical Applications: Present, Potentials, and Future Challenges, *Applied Spectroscopy Reviews*, 46, 1–37 (2011). DOI: 10.1080/05704928.2010.520178
8. F. Wang, Y. Cheng, Q. Xue, Q. Wang, R. Liang, J. Wu, J. Sun, C. Zhu, Q. Li, Techniques to enhance the photoacoustic signal for trace gas sensing: A review, *Sensors and Actuators A: Physical*, 345, 113807 (2022). DOI:10.1016/j.sna.2022.113807
9. A. Sampaolo, P. Patimisco, M. Giglio, A. Zifarelli, H. Wu, L. Dong, V. Spagnolo, Quartz-enhanced photoacoustic spectroscopy for multi-gas detection: A review, *Analytica Chimica Acta*, 1202, 338894 (2022). DOI:10.1016/j.aca.2021.338894
10. H. P. Wu, L. Dong, H. D. Zheng, Y. J. Yu, W. G. Ma, L. Zhang, W. B. Yin, L. T. Xiao, S. T. Jia, F. K. Tittel, Beat Frequency Quartz-Enhanced Photoacoustic Spectroscopy for Fast and Calibration-Free Continuous Trace-Gas Monitoring, *Nature Communications*, 8, 15331 (2017). DOI:10.1038/ncomms15331
11. K. Wilcken, J. Kauppinen, Optimization of a Microphone for Photoacoustic Spectroscopy, *Applied Spectroscopy*, 57, 1087–1092 (2003). DOI:10.1366/00037020360695946
12. J. Peltola, T. Hieta, M. Vainio, Parts-per-Trillion-Level Detection of Nitrogen Dioxide by Cantilever-Enhanced Photo-Acoustic Spectroscopy, *Optics Letters*, 40, 2933–2936 (2015) DOI:10.1364/OL.40.002933.
13. M. Lukić, Ž. Čojbašić, M. D. Rabasović, D. D. Markushev, Computationally intelligent pulsed photoacoustics, *Measurement Science and Technology* 25, 125203 (2014). DOI:10.1088/0957-0233/25/12/125203.
14. M. Lukić, Ž. Čojbašić, D. D. Markushev, Trace gases analysis in pulsed photoacoustics based on swarm intelligence optimization, *Optical and Quantum Electronics* 54, 674. (2022). DOI:10.1007/s11082-022-04059-y.
15. K. Lj. Djordjević, S. P. Galović, M. N. Popović, M.V. Nešić, I. P. Stanimirović, Z. I. Stanimirović, D. D. Markushev, Use Neural Network in Photoacoustic Measurement of Thermoelastic Properties of Aluminum foil, *Measurement* 199, 111537 (2022). DOI: 10.1016/j.measurement.2022.111537.
16. K. Lj. Djordjević, M. I. Jordović-Pavlović, Ž.M. Čojbašić, S. P. Galović, M. N. Popović, M. V. Nešić, D. D. Markushev, Influence of data scaling and normalization on overall neural network performances in photoacoustics, *Optical and Quantum Electronics*, 54, 501 (2022). DOI:10.1007/s11082-022-03799-1
17. M. Nesić, M. Popović, S. Galović, Developing the Techniques for Solving the Inverse Problem in Photoacoustics. *Atoms*. 7, 24 (2019) DOI:10.3390/atoms7010024.
18. A. Hauptmann, B. T. Cox, Deep learning in photoacoustic tomography: current approaches and future directions, *Journal of Biomedical Optics*, 25, 112903 (2020). DOI:10.1117/1.JBO.25.11.112903
19. K. M. Beck, R. J. Gordon, The vibrational relaxation of highly excited SF₆ by Ar, *Chemical Physics*, 87, 5681 (1987). DOI:10.1063/1.453736.
20. K. M. Beck, R. J. Gordon, Theory and application of time-resolved optoacoustics in gases, *The Journal of Chemical Physics*, 89, 5560 (1988). DOI:10.1063/1.455562.
21. R. T. Bailey, F. R. Cruickshank, R. Guthrie, D. Pugh, I. J. M. Weir, Short time - scale effects in the pulsed source thermal lens, *Molecular Physics* 48, 81-95 (1983). DOI:10.1080/00268978300100061.
22. J. Gajević, M. Stević, J. Nikolić, M. Rabasović, D. Markushev: Global warming and SF₆ molecule, *Facta Universitatis, Series: Physics, Chemistry and Technology*, 4, 57 – 69 (2006). DOI:10.2298/FUPC0601057G.
23. M. D. Rabasović, D. D. Markushev, J. Jovanović-Kurepa, Pulsed photoacoustic system calibration for highly excited molecules, *Meas. Sci. Technol.* 17, 1826-1837 (2006). DOI:10.1088/0957-0233/17/7/022.

24. M. D. Rabasović, J. D. Nikolić, D. D. Markushev Pulsed photoacoustic system calibration for highly excited molecules: II. Influence of the laser beam profile and the excitation energy decay. *Measurement Science and Technology*, 17, 2938-2944 (2006). DOI:10.1088/0957-0233/17/11/011.
25. S. D. Russo, A. Sampaolo, P. Patimisco, G. Menduni, M. Giglio, C. Hoelzl, V. M.N. Passaro, H. Wu, L. Dong, V. Spagnolo, Quartz-enhanced photoacoustic spectroscopy exploiting low-frequency tuning forks as a tool to measure the vibrational relaxation rate in gas species, *Photoacoustics*, 21, 100227 (2021). DOI: 10.1016/j.pacs.2020.100227.
26. M. D. Rabasović, J. D. Nikolić, D. D. Markushev, Simultaneous determination of the spatial profile of the laser beam and vibrational-to-translational relaxation time by pulsed photoacoustics, *Applied Physics B*, 88, 309-315 (2007). DOI:10.1007/s00340-007-2697-4.
27. M. D. Rabasović, D. D. Markushev, Laser beam spatial profile determination by pulsed photoacoustics: exact solution, *Measurement Science and Technology*, 21, 065603 (2010). DOI:10.1088/0957-0233/21/6/065603.
28. S. Mallidi, S. Emelianov, Photoacoustic technique to measure beam profile of pulsed laser systems, *Review of Scientific Instruments*, 80, 054901-1-054901-5 (2009). DOI:10.1063/1.3125625.
29. L. Lamainière, R. Courchinoux, N. Roquin, R. Parreault, T. Donval, Laser-induced damage of high power systems: phenomenology and mechanisms Proc. SPIE 11063, Pacific Rim Laser Damage: Optical Materials for High-Power Lasers 1106309, (2019). DOI:10.1117/12.2537106.
30. M. Lukić, Ž. Čojbašić, D. Markushev: Simulated Annealing Optimization for Inverse Problem Solving of Trace Gases Detection by Infrared Pulsed Photoacoustic, *Proceedings of 15 International conference on applied electromagnetics, IIEC 2021*, 121-124, (2021), Niš, Serbia ISBN:978-86-6125-241-9.
31. K.L. Du, M.N.S. Swamy, Neural Networks and Statistical Learning, Springer-Verlag London 2014.
32. A.P. Engelbrecht, Computational Intelligence, 2nd edition. John Wiley and Sons 2007.
33. M. Lukić, Ž. Čojbašić, M. Rabasović, D. Markushev, D. Todorović, Computational intelligence based simultaneous determination of the spatial profile of the laser beam and vibrational-to-translational relaxation time by pulsed photoacoustics, *Facta Universitatis, Series: Physics, Chemistry and Technology* 10, 1-12 (2012). DOI: 10.2298/FUPCT1201001L.
34. M.Lukić, Ž. Čojbašić, M. Rabasović, D. Markushev, D. Todorović: Genetic algorithms application for the photoacoustic signal temporal shape analysis and energy density distribution calculation, *International Journal of Thermophysics*, 34, 1466-1472 (2013). DOI 10.1007/s10765-013-1529-5.
35. M. Lukić, Ž. Čojbašić, M. Rabasović, D. Markushev, D. Todorović, Neural Networks-Based Real-Time Determination of the Laser Beam Spatial Profile and Vibrational-to-Translational Relaxation Time Within Pulsed Photoacoustics, *Int J Thermophys* 34:1795–1802 (2013) DOI: 10.1007/s10765-013-1507-y
36. J.D. Lambert, *Vibrational and Rotational Relaxation in Gases*, Oxford University Press (1977).
37. M. Lukić, Ž. Čojbašić, D. Markushev, Machine learning based determination of photoacoustic signal parameters for different gas mixtures, *Book of Abstracts, ICPPP21 - International Conference on Photoacoustic and Photothermal Phenomena*, 365-366 (2022), Bled, Slovenia, <https://heyzine.com/flip-book/ae82c5ef9b.html#page/376>
38. J.H. Holland, *Adaptation in natural and artificial systems*, MIT Press, Massachusetts, 1992.
39. D.E. Goldberg, *Genetic algorithms in search, optimization, and machine learning*. Addison-Wesley Longman Publishing Co.1989, Boston.
40. D.T. Pham and D. Karaboga, *Intelligent optimisation techniques*, Springer-Verlag London, 2000.
41. S. Kirkpatrick, C. D. Gelatt, M. P. Vecchi, Optimization by Simulated Annealing, *Science*, **220**, 671-680 (1983).
42. K. L. Du, M. N. S. Swamy, *Simulated annealing. Search and Optimization by Metaheuristics*, Springer International Publishing, 2016, AG Switzerland
43. E. G. Talbi, *Metaheuristics - From design to implementation*, John Wiley & Sons, 2009, New Jersey.

PRIMENA VEŠTAČKE INTELIGENCIJE U FOTOAKUSTICI GASOVA

Fotoakustička spektroskopija je moćna, nedestruktivna, visoko osetljiva tehnika, koja se široko primenjuje u atmosferskim, industrijskim, biomedicinskim i istraživanjima u životnoj sredini. U ovom radu je prikazana primena veštačke inteligencije u fotoakustičkoj spektroskopiji gasova. Veštačka inteligencija je veoma uspešna, efikasna i perspektivna tehnika za određivanje parametara fotoakustičkog signala u realnom vremenu, povezanim sa relaksacijom, toplotnim i drugim fizičkim karakteristikama različitih sredina (tj. za rešavanje inverznog problema). S ciljem povećanja osetljivosti i

selektivnosti fotoakustičkog metoda, za istovremeno određivanje parametara fotoakustičkog signala u realnom vremenu: vibraciono-translacionog relaksacionog vremena i poluprečnika laserskog profila, korišćena je višeslojna perceptronska neuronska mreža. Takođe, za rešavanje problema nalaženja optimalnih vrednosti ovih parametara fotoakustičkog signala, korišćena su dva metaheuristička algoritma: genetski algoritmi i algoritam simuliranog žarenja. Rezultati dobijeni metodom veštačke inteligencije testirani su na skupu eksperimentalnih signala generisanih u gasnoj smeši (SF₆+Ar). Razmatrane su potencijalne prednosti primene metoda veštačke inteligencije, ali i nedostaci.

Ključne reči: fotoakustička spektroskopija, veštačke neuronske mreže, vibraciono-translaciono relaksaciono vreme, poluprečnik lasarskog snopa, genetski algoritmi, simulirano žarenje.